

Supplementary Material: Parallel QND measurement tomography of multi-qubit quantum devices

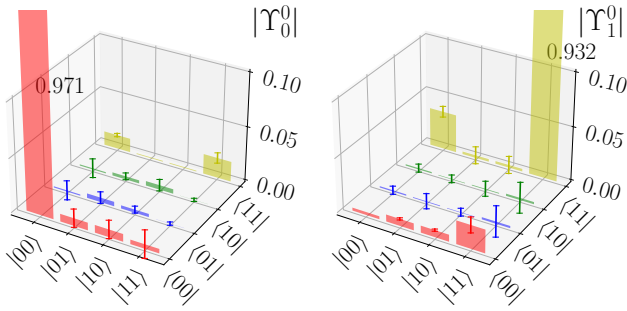
L. Pereira¹, J.J. García-Ripoll¹, and T. Ramos¹

¹ *Instituto de Física Fundamental IFF-CSIC, Calle Serrano 113b, Madrid 28006, Spain*

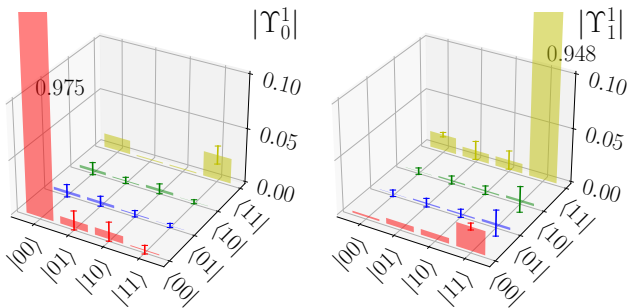
SUPPLEMENTARY FIGURES

I.- All experimental single-qubit Choi matrices

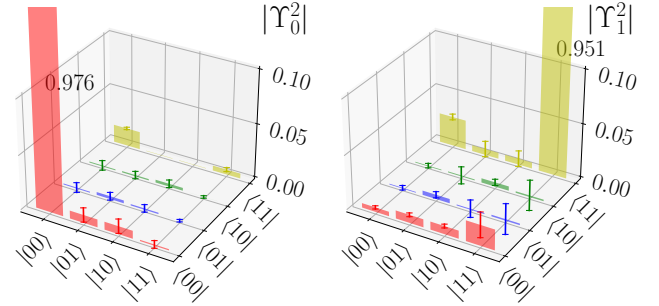
In this section, we show the absolute value of all the reconstructed single-qubit Choi matrices Υ_n^α for all possible measurement outcomes $n = 0, 1$ of every qubit $\alpha = 0, \dots, 6$ of the *ibm_perth* chip shown in Figure 1(e) of the main text. All the definitions, calculation procedures, and error treatments are explained in the main text and methods.



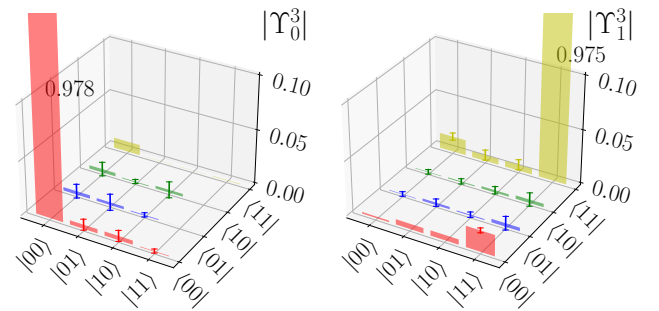
Supplementary Figure 1. Absolute value of the reconstructed Choi matrices Υ_n^0 for a measurement on qubit $\alpha = 0$. Error bars are the standard deviation estimated with 5 realizations of the experiment.



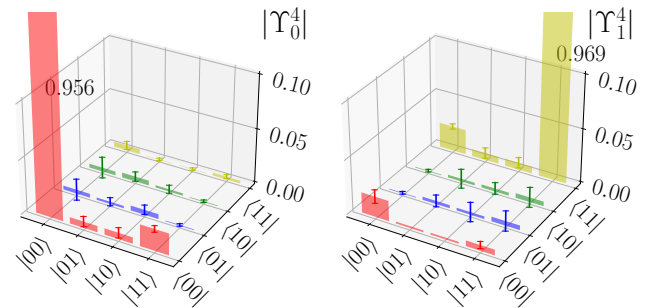
Supplementary Figure 2. Absolute value of the reconstructed Choi matrices Υ_n^1 for a measurement on qubit $\alpha = 1$. Error bars are the standard deviation estimated with 5 realizations of the experiment.



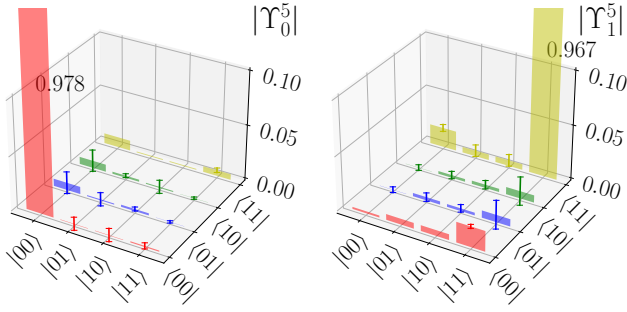
Supplementary Figure 3. Absolute value of the reconstructed Choi matrices Υ_n^2 for a measurement on qubit $\alpha = 2$. Error bars are the standard deviation estimated with 5 realizations of the experiment.



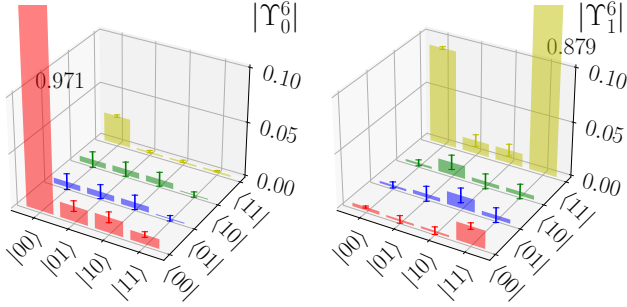
Supplementary Figure 4. Absolute value of the reconstructed Choi matrices Υ_n^3 for a measurement on qubit $\alpha = 3$. Error bars are the standard deviation estimated with 5 realizations of the experiment.



Supplementary Figure 5. Absolute value of the reconstructed Choi matrices Υ_n^4 for a measurement on qubit $\alpha = 4$. Error bars are the standard deviation estimated with 5 realizations of the experiment.



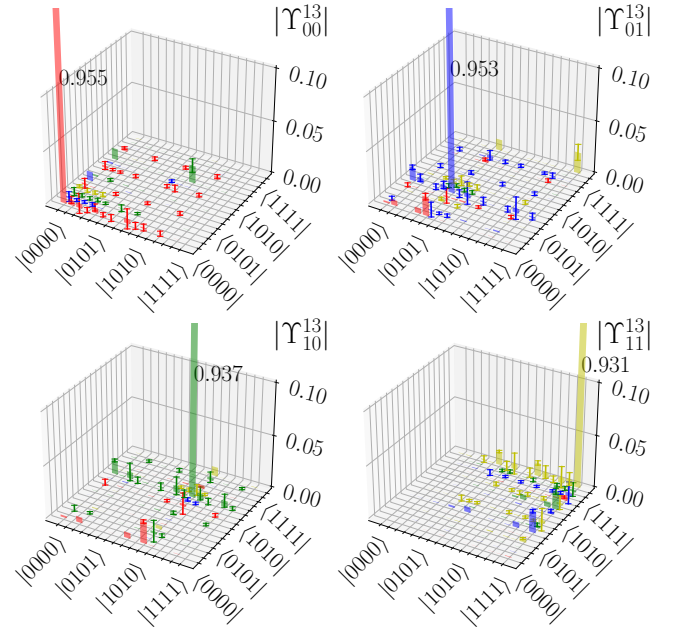
Supplementary Figure 6. Absolute value of the reconstructed Choi matrices Υ_n^5 for a measurement on qubit $\alpha = 5$. Error bars are the standard deviation estimated with 5 realizations of the experiment.



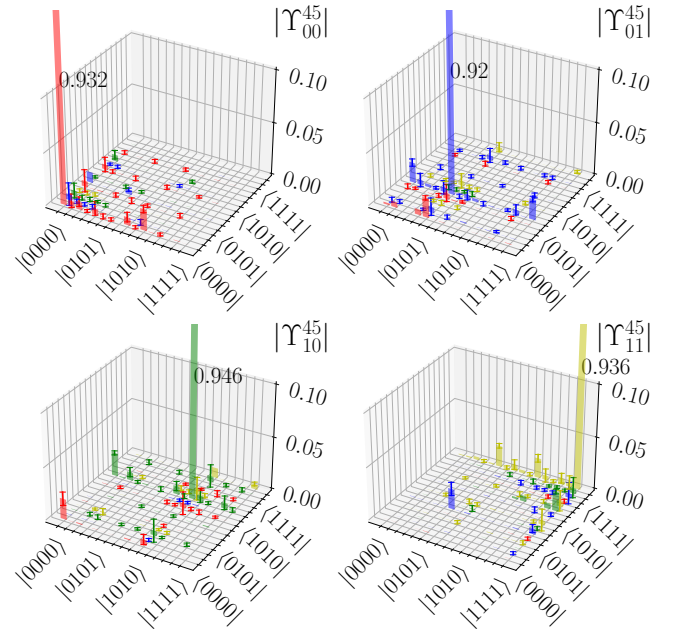
Supplementary Figure 7. Absolute value of the reconstructed Choi matrices Υ_n^6 for a measurement on qubit $\alpha = 6$. Error bars are the standard deviation estimated with 5 realizations of the experiment.

II.- All experimental two-qubit Choi matrices

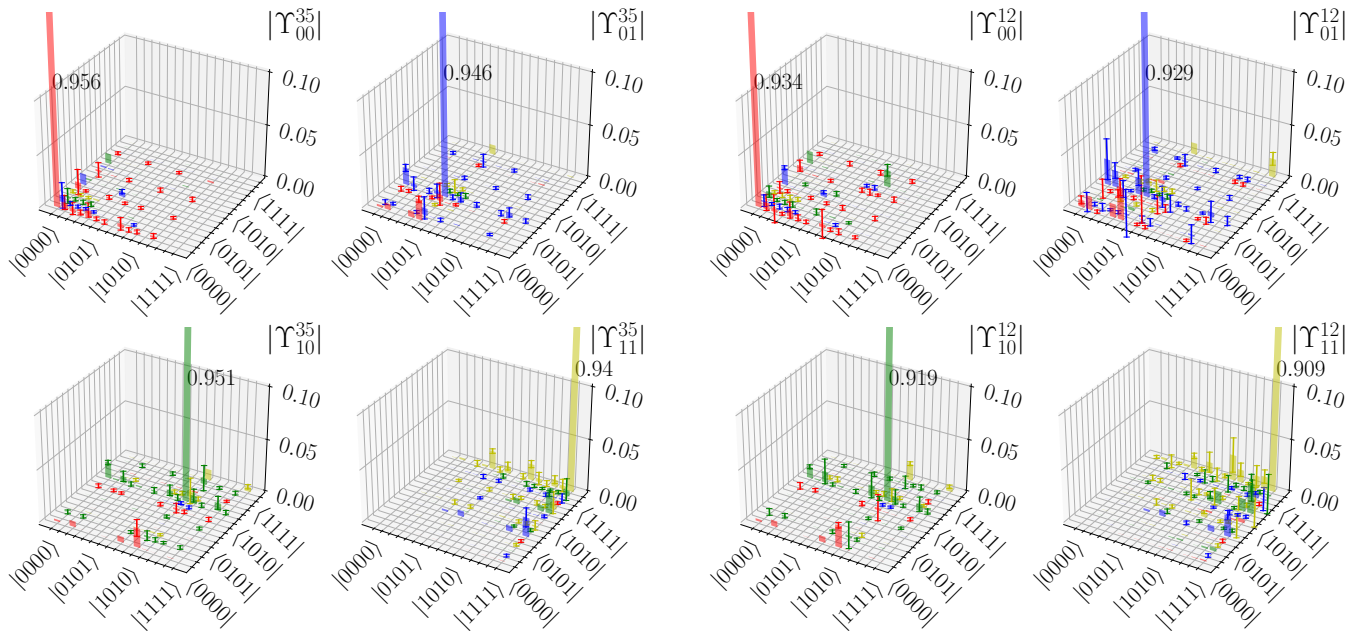
In this section, we show the absolute value of all the reconstructed two-qubit Choi matrices $\Upsilon_{nm}^{\alpha\beta}$ for the four possible measurement outcomes $(n, m) \in \{(0, 0), (0, 1), (1, 0), (1, 1)\}$ of every pair of physically connected qubits $(\alpha, \beta) \in \{(0, 1), (1, 2), (1, 3), (3, 5), (4, 5), (5, 6)\}$ of the *ibm_perth* chip shown in Fig. 1(e) of the main text. All the definitions, calculation procedures, and error treatments are explained in the main text and methods. We also show the Choi matrices of the joint measurements of qubit $\alpha = 3$ with respect to all other pairs in the device, which were used to calculate Fig. 4(b) of the main text.



Supplementary Figure 8. Absolute value of the reconstructed Choi matrices Υ_{nm}^{01} for a measurement on the two qubits $(\alpha, \beta) = (1, 3)$. Error bars are the standard deviation estimated with 5 realizations of the experiment.

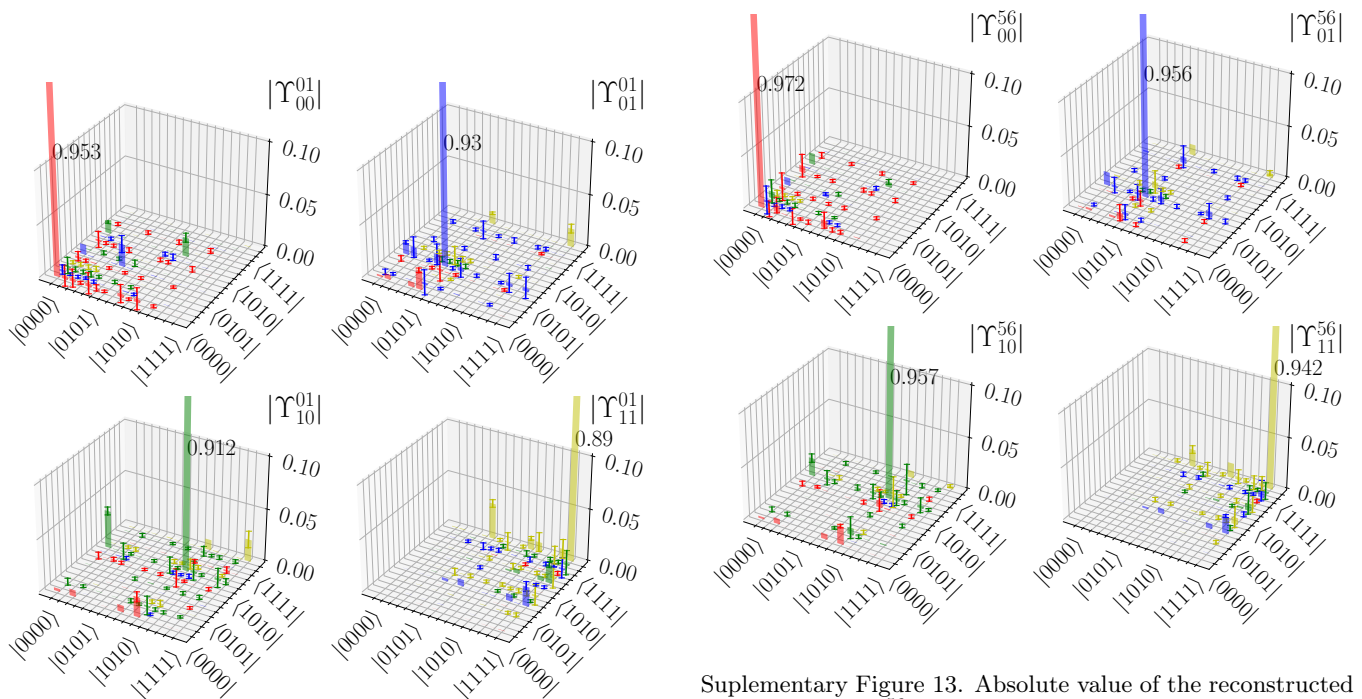


Supplementary Figure 9. Absolute value of the reconstructed Choi matrices Υ_{nm}^{12} for a measurement on the two qubits $(\alpha, \beta) = (4, 5)$. Error bars are the standard deviation estimated with 5 realizations of the experiment.



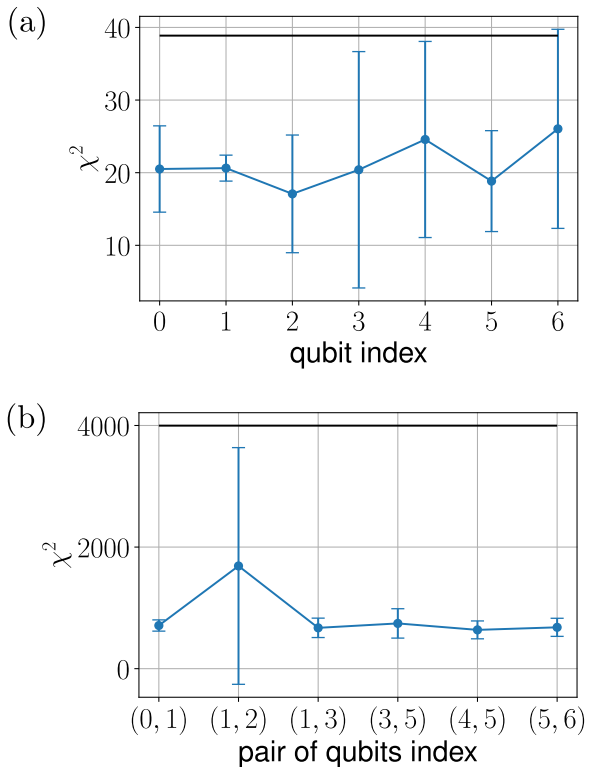
Supplementary Figure 10. Absolute value of the reconstructed Choi matrices Υ_{nm}^{13} for a measurement on the two qubits $(\alpha, \beta) = (3, 5)$. Error bars are the standard deviation estimated with 5 realizations of the experiment.

Supplementary Figure 12. Absolute value of the reconstructed Choi matrices Υ_{nm}^{45} for a measurement on the two qubits $(\alpha, \beta) = (1, 2)$. Error bars are the standard deviation estimated with 5 realizations of the experiment.



Supplementary Figure 11. Absolute value of the reconstructed Choi matrices Υ_{nm}^{35} for a measurement on the two qubits $(\alpha, \beta) = (0, 1)$. Error bars are the standard deviation estimated with 5 realizations of the experiment.

Supplementary Figure 13. Absolute value of the reconstructed Choi matrices Υ_{nm}^{56} for a measurement on the two qubits $(\alpha, \beta) = (5, 6)$. Error bars are the standard deviation estimated with 5 realizations of the experiment.



Supplementary Figure 14. Goodness-of-fit of the single- and two-qubit QND-MT of *ibm_perth* device. All the χ^2 values are within the 95% confidence threshold indicated by the black horizontal line. Error bars are the standard deviation estimated with 5 realizations of the experiment.

SUPPLEMENTARY METHODS

I.- Goodness-of-fit via χ^2 -test

Let be $c(mn|jk)$ the counts obtained from the QND-MT of measurement process, which are used to obtain an estimator $\{\hat{Y}_n\}$. The goodness-of-fit χ^2 test for this data reads

1. Compute the predicted probabilities,

$$p(nm|jk) = \text{Tr}[(\hat{\mathcal{F}}_j^\dagger(\hat{\Pi}_m) \otimes \hat{\mathcal{F}}_k(\hat{\rho})^T)\hat{Y}_n], \quad (1)$$

where $\{\hat{\rho}, \hat{\Pi}_n, \hat{\mathcal{F}}_j\}$ is the gate set estimated with GST.

2. Compute the test statistic,

$$\chi^2 = \sum_{j=1}^M \frac{(c_j - N_s p_j)^2}{N_s p_j}, \quad (2)$$

where N_s is the number of shots used to evaluate the probabilities.

3. Set an error probability q (typically as 0.05) and compute χ_q^2 , implicitly defined by

$$q = \int_{\chi_q^2}^{\infty} P_r(x) dx, \quad (3)$$

where P_r is the probability density function of a χ^2 variable with mean r ,

$$P_r(x) = \frac{x^{(r-2)/2} e^{-x/2}}{2^{r/2} \Gamma(\frac{r}{2})}. \quad (4)$$

The mean value r is given by

$$r = \left(\begin{array}{c} \text{number of} \\ \text{independent} \\ \text{probabilities} \end{array} \right) - \left(\begin{array}{c} \text{number of} \\ \text{parameters} \\ \text{of the model} \end{array} \right). \quad (5)$$

For a N -qubit detector, this mean value is given by

$$r_N = 18^N \times (4^N - 1) - (2^N \times 16^N - 4^N). \quad (6)$$

Each term from left to right corresponds to: number of circuit (18^N), independent probabilities per circuit ($4^N - 1$), number of free parameters of the Choi matrices ($2^N \times 16^N$), and completeness constraint (4^N). For the cases of single- and two-qubits detectors, these are $r_1 = 26$ and $r_2 = 3852$, respectively.

4. Reject the hypothesis if $\chi^2 \geq \chi_q^2$.

We apply this procedure to quantify the goodness-of-fit of our characterization of the *ibm_perth* device with QND-MT presented. As shown in Supplementary Figure 14, both single- (a) and two-qubit (b) characterizations have a χ^2 value below the threshold χ_q^2 (black horizontal line) and therefore are consistent with the experimental data with confidence 95% ($q = 0.05$).